Heat Extrusion Unit for Ocean Cleaning of Plastic Debris by Melting for Volume Reduction

Mr. Jacob Daniel Belmontes, California State University, Los Angeles

Education: Bachelor of Science Mechanical Engineering, California State University, Los Angeles; Employment: Manufacturing Engineer at Donaldson Aerospace and Defense (2017 - 2018), Manufacturing Engineer II at Aerojet Rocketdyne (2018 - present); Honors: Cum Laude Honors Graduate; Academic Organization: Tao Beta Pi Engineering Honors Society (2016 – Present)

Juan Jose Dominguez, California State University, Los Angeles

Education: B.S Mechanical Engineering California State University, Los Angeles

Mr. Nhat Minh Ly, California State University, Los Angeles

Education: - Graduated at Cal State LA with Bachelors of Science in Mechanical Engineer. Experience: - Military services in United State Army Reserve for 6 years. - Jr. Mechanical engineer at Lambda Research Optics.

Mr. Mathew Rafael Rojas, California State University, Los Angeles

Education: B.S Mechanical Engineering California State University Los Angeles (2014-2018)

Ivan Juarez, California State University, Los Angeles

Education: B.S Mechanical Engineering Cal State LA (2013-2018) Work Experience: Associate Project Engineer (Los Angeles Unified School District)

Mr. Anthony Po-Hong Wong, California State University, Los Angeles

An undergraduate of Mechanical engineering from the California State University, Los Angeles with some experience in the field. Specialty lies with automation and controls.

Heat Extrusion Unit for Ocean Cleaning of Plastic Debris by Melting for Volume Reduction

Abstract

The proceeding information provides predicted results provided by mathematical modeling, functionality, and equations used to mechanically operate and design a system that will collectively process plastic ocean debris into elasticized solid lumps for means of transportation out of, and away from ocean waters.

The preliminary chosen design was a combination of a cylindrical compactor and heating induced elements. The final design, titled Heat Extrusion Unit; included a pipe of pre-determined length that houses the driving mechanism, an Auger to transport plastic material forward, an electric DC motor to rotate the Auger, a Hopper to chamber plastic debris for processing, Heating Bands to phase change plastic from solid-to-liquid, and an exit nozzle for processed plastic extrusion.

Conduction Heat Transfer and Heat Transfer Coefficient equations for a steel pipe were applied in conjunction with the Logarithmic Mean Temperature Difference to determine both the minimum working distance of heated pipe length needed, and the minimum power required to phase change plastic. The Mass Flow Rate equation was used to determine the motor's torque and angular velocity for material transportation. Based on Auger geometry and mass flow rate variables, calculations for theoretical material processing rates were obtained.

This project began with three imposed upon requirements: mass constraint, power allotment, and corrosion resistant materials. Based on computer aided design, mathematical models, and material research, final results for the design's mass, power usage, and chosen materials were 24.2kg, 678Wh, and 316L stainless steel respectively; all of which were within system requirements. Use of the Conduction Heat Transfer and Heat Transfer Coefficient equations aided in providing a numerical reference to identify a 6.21×10^{-1}m of minimum pipe length working distance required to successfully process plastic material waste.

The final analysis determining feasibility of the design for practical operation has been achieved. With collected data from an assembled and functional Heat Extrusion Unit prototype, the interior and exterior, heating system, mechanical system, and electrical system have been mathematically modeled and demonstrated to show processing behavior and its intended use.

Nomenclature:

Symbol	Description	Unit	Symbol	Description	Unit
$\left[\frac{\delta p}{\delta z}\right]$	Pressure Gradient	kPa/m	ΔT	Change in Temperature	˚C
ΔT_1	Change in Temperature at 1	˚C	ΔT_2	Change in Temperature at 2	˚C
ΔT_{lm}	Log Mean Temperature Difference	˚C	η	Shear Viscosity	Pa·s
θ_b	Helix Angle at Barrel Wall	◦	ρ_m	Melt Density	kg/m^3
ω	Angular Velocity	rev/m	c_p	Specific Heat Capacity	J/kgK
D_b	Inner Diameter of Barrel	m	dT	Change in Material Temperature	˚C
F_d	Shape Factor for Plane Couette Flow	-	F_p	Shape Factor for Pressure Flow	-
H	Channel Depth	m	k	Thermal Conductivity	W/m^{2}K
k_{PET}	Thermal Conductivity of PET	W/m^{2}K	k_{ST}	Thermal Conductivity of Steel	W/m^{2}K
L	Length	m	L_f	Latent Heat of Fusion	kJ/kg
$\dot{m}$	Mass Flow Rate	kg/s	N	Revolution Rate	rev/s
P	Power	W	p	Number of Flight Starts	-
$\dot{q}_{cp}$	Specific Heat Capacity Heat Flow	kJ/s	$\dot{q}_{L_f}$	Latent Heat Flow	kJ/s
$\dot{Q}_{md}$	Mass Rotational Flow	kg/s	$\dot{Q}_{mp}$	Mass Pressure Flow	kg/s
$\dot{q}_r$	Radial Heat Flow Rate	kJ/s	q_r	Radial Heat Flow	kJ
$\dot{Q}_{total}$	Total Heat Flow	kJ/s	r_1	Radius of Auger	m
r_2	Radius of Inner Wall of Cylindrical Chamber	m	r_3	Radius of Outer Wall of Cylindrical Chamber	m
T	Torque	Nm	V_{bz}	Screw Velocity at Barrel Wall	m/s
W	Average Channel Width	m			

Introduction, Background, and Societal Impacts:

The disposal of plastic waste into our oceans is currently considered a major concern of modern society. In ocean waters, plastics do not fully break down; but only degrade to smaller pieces which affects ecosystems in many harmful ways [1]. Mistaking these plastics as a source of food, marine life often consumes these degraded plastics and passes them further into the food chain [2]. Prior to ingestion, byproducts such as Bisphenol and Antimony (BPA) begin to develop due to exposure from the Sun's radiation. Moreover, these carcinogenic micro-sized plastics can end up in our bodies by fish-foods that contain these plastics, and lead to chronic illnesses such as cancer. They also negatively impact the growth and development of marine life by accumulating into large "trash islands", the most famous being the Great Pacific garbage patch.

Researching methods to process and recycle plastic has, therefore; been one of the most important challenges for scientists and engineers worldwide for the past seven-decades. Plastics, especially polyethylene, have very strong and stable atomic bond structures which require a minimum of three hundred to a thousand years to naturally decompose [1]. Without appropriate means to handle this crisis, further accumulation has already reached dangerous levels.

As a result, a solution was developed, tested, and is ready for deployment to combat the accumulation of ocean plastic waste. The primary function of the manufactured design is to combine micro-sized plastic pieces into single elastized-lumps for means of transportation out of, and away from ocean waters.

Project Scope and System Requirements:

The goal was to design a system that is capable of processing plastic debris ranging from 0.1mm to 5mm in size, and at a minimum expected processing rate of 3.63kg/h. In addition, this plastic processing system could not exceed a total weight of 50kg, and an overall power consumption of less than or equal to 800Wh. Since location of this system is designated far out into ocean waters, system components would require a material composition that is resistant to the salinity of the ocean [3].

Preliminary Design:

In the early 1980's, NASA began researching methods to reduce waste that occurred during long-term space explorations in efforts to minimize the amount of valuable working space and living quarters that waste occupied [4]**.** For close to two decades, NASA's engineers were convinced that their most efficient waste management process depended on the use of mechanical energy. Their proposed design was called The Compress Melt Unit (CMU); however, the solution that the engineers at NASA provided came at several costs which included but were not limited to, short-term operation lifetime before failure, excessive electrical power consumption, routine maintenance, and much more.

In 2003, the U.S Navy joined NASA's CMU research program and began experimenting with a Heat Melt Compactor (HMC) [4]**.** The purpose of the HMC was to use heat application along

with hand-driven mechanical energy to soften waste at specific glass transition temperatures[1], which caused materials to bind together and form solid conformed shapes. The HMC proved to be the most efficient processing method, and as of today; it is currently being used on all man piloted space explorations, The International Space Station, and all U.S. naval ships.

The HMC design provided a practical approach to develop a system for the processing of ocean plastic debris. However, in order for the HEU to operate as intended; changes in the HMC concept needed a substitution for its man-powered compression process. As seen in Figure 1 below, applying heat temperatures that ranged from (150 to 180)°C [4] generated possibilities to hand-compress plastic waste at manageable pressures.

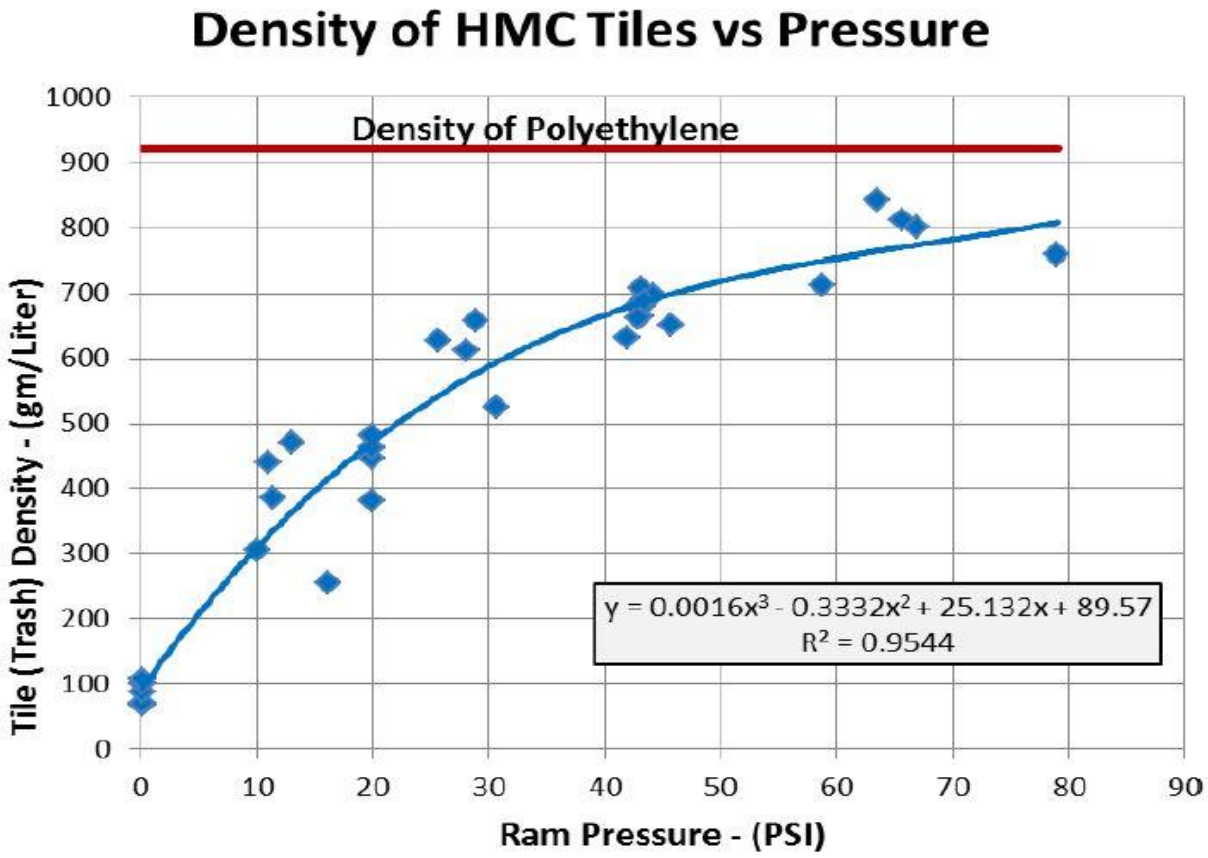

Figure 1 Hand-Driven Compression Data [5]

To achieve functional success, two challenges were presented during conceptual design for a system that is capable of processing ocean plastic. The first challenge was the need to substitute the HMC's hand-compression method by use of a linear actuator, and the second challenge was to integrate a heating process to soften plastic debris. Figure 2 below shows the preliminary design choice for a Heat Extrusion Unit (HEU).

[1] Temperature of solid plastic when material develops a phase changed thin film layer of liquid [5]

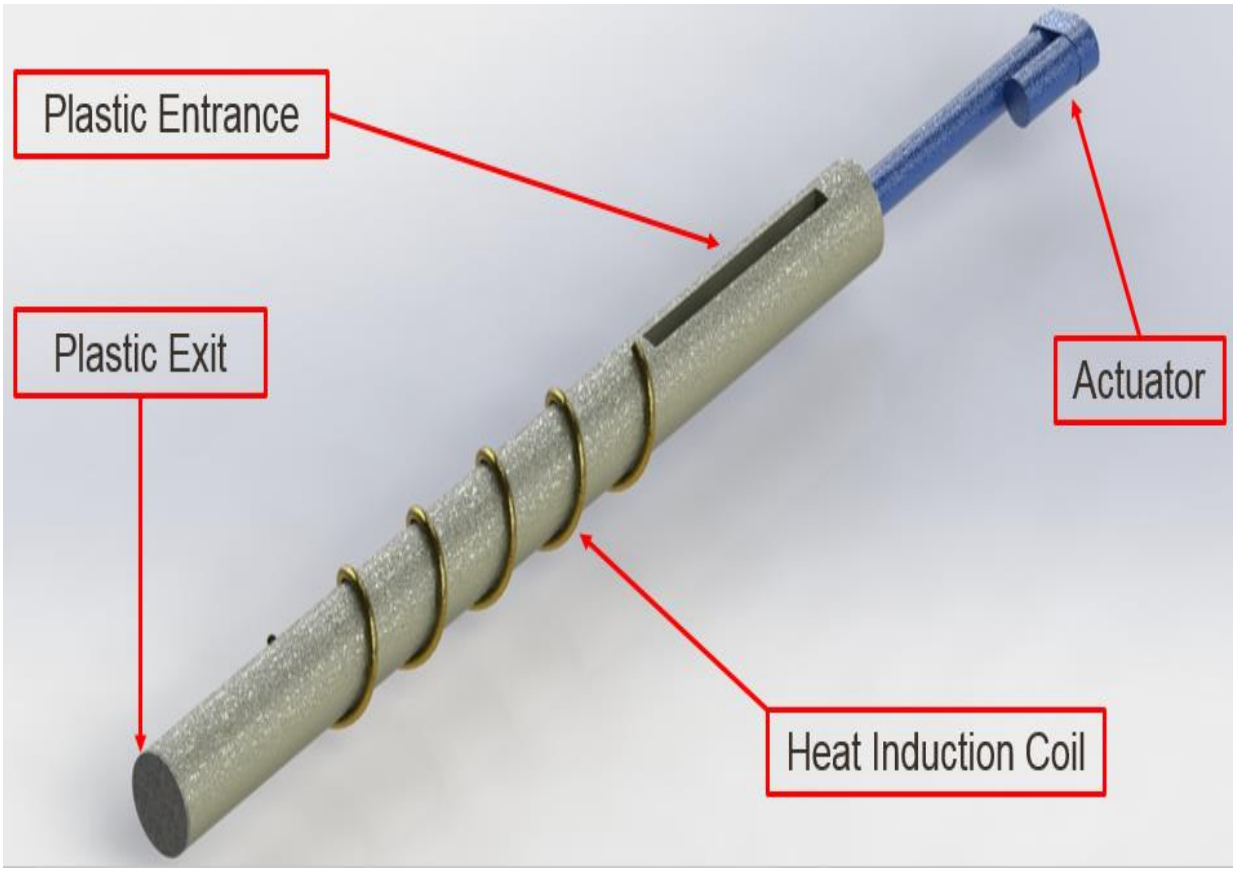

Figure 2 Preliminary Design for a Plastic Processing System

The incorporation of a Heat Induction Coil was initially chosen to induce heat by form of non-contact heat transfer caused by electromagnetic induction. However, use of a heating coil would complicate the design since it would require a water pump along with its own power supply. Another complication with the heating coil option was that the minimum power consumption of the coil was 1.5kWh, which exceeded this project's maximum power constraint.

In addition, it was determined by calculations that a customized actuator was needed to generate the force required in order to meet the project's mass flow rate system requirement. Choosing to proceed with this form of processing was impractical due to production costs. Through analysis of pros and cons, safety, efficiency, practicality, and processing methods to generate the least out-of-pocket expense, led to the changes that were implemented in the final design of this project.

Further research was conducted in order to redesign the compression and heating aspects of the system. After much deliberation, it was determined that heating bands were a much more affordable option, both in price and power consumption. The heating bands would also simplify the design of the heating system since the heating bands did not require a water pump or its own power supply. Finally, it was discovered that the function of an actuator could be similarily performed by an Archimedes Screw connected with an electric motor at a significantly reduced cost. The Archimedes Screw would be able to drive plastic toward the heated section of the system while simultaneously compressing and processing it through the Extrusion Nozzle.

Mathematical Model:

Pipe Length

Modeling the Cylindrical Chamber to identify the necessary pipe length was the first challenge to overcome when designing a prototype. Successfully processing plastic was dependent on interior and exterior geometry, temperature, and power; all of which was modeled using Fourier's Law [6] in the radial direction:

$$q_r = \frac{2\pi kL(\Delta T)}{\ln\left(\frac{r_2}{r_1}\right)} \quad \text{Eq.1}$$

Polyethelene (PET) was specifically targeted as the necessary glass transition temperature to reach due to its large density. By qualitative reasoning, all other plastics with densities less than PET would experience solid-to-liquid phase changes, as internal temperature rose to 110°C. In order to reach 110°C, q_r was the resulting summation of latent heat of fusion q_{L_f} [6], and specific heat capacity q_{cp} [6]:

$$\dot{q}_{L_f} = \dot{m}L_f \quad \text{Eq.2}$$

$$\dot{q}_{cp} = \dot{m}c_P dT \quad \text{Eq.3}$$

Due to variances in external, Hopper entrance, internal Cylindrical Chamber, and Extrusion Nozzle exit temperatures; incorporating the log mean temperature equation [6] was needed.

$$\Delta T_{lm} = \frac{\Delta T_1 - \Delta T_2}{\ln(\frac{\Delta T_1}{\Delta T_2})} \quad \text{Eq.4}$$

Minimum working distance

In order to accurately model the HEU using conduction heat transfer concepts, it was necessary to assume that the pipe was fully occupied by the combination of plastic and Auger. Under this assumption, including new constants such as thermal conductivity coefficients k_{PET} and k_{ST}, outer Auger radius r_1, inner Cylindrical Chamber wall r_2, and outer Cylindircal Chamber wall r_3 were incorporated. Along with the new Radial Heat Flow Rate term $\dot{q}_r$, algbracially rearraging the equation allowed for length L to be obtained.

$$L = \frac{\left[(2\pi k_{ST})\left(\ln\frac{r_3}{r_2}\right)\right] + \left[(2\pi k_{PET})\left(\ln(\frac{r_2}{r_1})\right)\right]}{\Delta T_{lm}}(\dot{q}_r) \quad \text{Eq.5}$$

With the length L set as a function of the preceding equation, and the temperature value at which PET Glass Transition Temperature occurs; the minimum working distance for pipe length geometry has been determined. The pipe length needed to achieve a state of liquidity for all plastic pieces occurs at the intersecting point between the solid blue and orange dashed lines as seen in Figure 3 below.

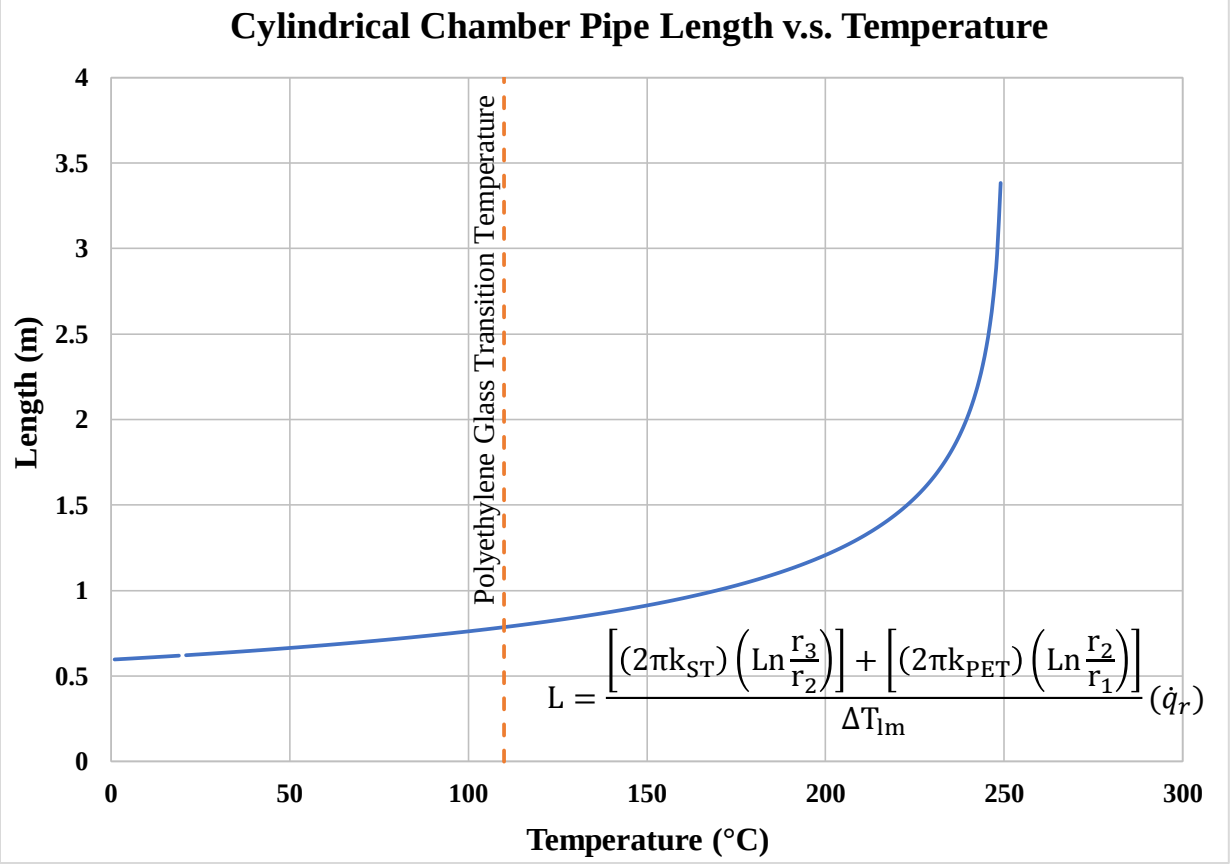

Figure 3 Plastic Processing Pipe Length

Mass Flow Rate

The ability to predict the amount of mass the HEU can produce was the next challenge encountered during prototype construction. Anticipating that the HEU would not operate under mass flow rate Steady-State[2] [7] conditions, theoretical mass flow rate production became dependent on two equations: mass rotational flow rate $\dot{Q}_{md}$, and mass pressure flow rate $\dot{Q}_{mp}$ [8]:

$$\dot{Q}_{md} = \frac{p\rho_m V_{bz} WHF_d}{2} \quad \text{Eq.6}$$

$$\dot{Q}_{mp} = \frac{p\rho_m WH^3 F_p}{12\eta}\left[\frac{\delta P}{\delta z}\right] \quad \text{Eq.7}$$

The difference between the preceding two equations yield the total mass flow rate $\dot{Q}_{total}$, as seen in Eq.8.

$$\dot{Q}_{total} = \dot{Q}_{md} - \dot{Q}_{mp} \quad \text{Eq.8}$$

[2] Mass flow rate Steady-State conditions are defined as an equal amount of mass entering and exiting a control volume over a period of time [7].

Each flow rate equation and its subsequent independent function V_{bz}, included a variety of constants from auger drill bit geometry, p, W, and H, cylinder pipe geometry D_b and θ_b; and PET density ρ_m. The remaining two constants F_d and F_p, were unitless correction factors that were given from within their respective equations. For purposes of simplification, the shear viscosity function η was also treated as a constant due to its negligible changes in magnitude.

$$V_{bz} = \pi N D_b cos\theta_b \quad \text{Eq.9}$$

Screw Velocity V_{bz} from Eq.9, was the dependent variable that posed the remaining challenge for mass flow rate modeling accuracy. V_{bz} was responsible for describing the velocity at which material traveled inside the Cylindrical Chamber. Upon algebraically rearranging the term *N* as seen in equation 10 below, motor output for Auger rotational speed was now determined.

$$N = \frac{V_{bz}}{\pi D_b cos\theta_b} \quad \text{Eq.10}$$

From revolutions per second *N*, to revolutions per minute ω, the resulting conversion provided Auger rotational speed which was utilized to determine the motor power requirement by equation 11.

$$\mathrm{P} = \mathrm{T}\omega \quad \text{Eq.11}$$

Final Design and Structural Overview:

Material Selection

In efforts to find a corrosive resistant choice of material for system requirements, three materials were considered from a long list of usable alloys: Aluminum Bronze, 17 – 4 PH, and 316SS.

Table 1 Material Properties

	Material		
Attribute	**Aluminum BronzeC95400 "9C"**	**17 - 4 PH Stainless Steel**	**316L Stainless Steel**
Melting Temp. (°C)	> 1000	> 1400	> 1300
Yield Strength (ksi)	32	145	30
Brinell Hardness	170	352	217
Weldability	Fair	Good	Good
Cost per Pound ($)	1.50*	0.68*	0.49*

With the HEU operating and idling at a temperature around 300°C, all three material choices as seen in Table 1 above offered a melting temperature allowance with a factor-of-safety close to three to four times greater than expected usage. Furthermore, with respect to material

* Cost-per-Pound market prices were obtained in November 2017

composition, all three materials provided a strong resistance to corrosion in a salt-rich oceanic environment. However, since cost of materials is always a concern in regards to manufacturing; the copper rich alloy Aluminum Bronze C95400 was quickly discarded due to its high cost, and lack of comparable mechanical properties. 17 – 4 PH and 316L Stainless Steel stood as the HEU's two remaining material choices, and although 17 – 4 PH was approximately 40 percent more expensive than 316L Stainless Steel; its price was easily justified by all of its categorical dominance in comparison to 316L Stainless Steel. The deciding factor between the two-steels came upon realization of an anticipated major concern. During plastic processing operations, heavy frictional contact would generate between Auger rotation and the inner walls of the Cylindrical Chamber. This contact would cause severe surface exposure as the Auger and cylinder wall scrapped and rubbed during processing. Further analysis concluded that keeping salt water out of the system while plastic entered the Hopper was practically impossible to avoid. 316L stainless steel became the choice of material for the HEU due to its two percent molybdenum additive component, good Brinell Hardness value, and good weldability ease for fabrication properties. Except for the Heat Bands, Auger, and Insulation as seen in Figure 4 below, all of the HEU's exterior components and fasteners are made using 316L Stainless Steel.

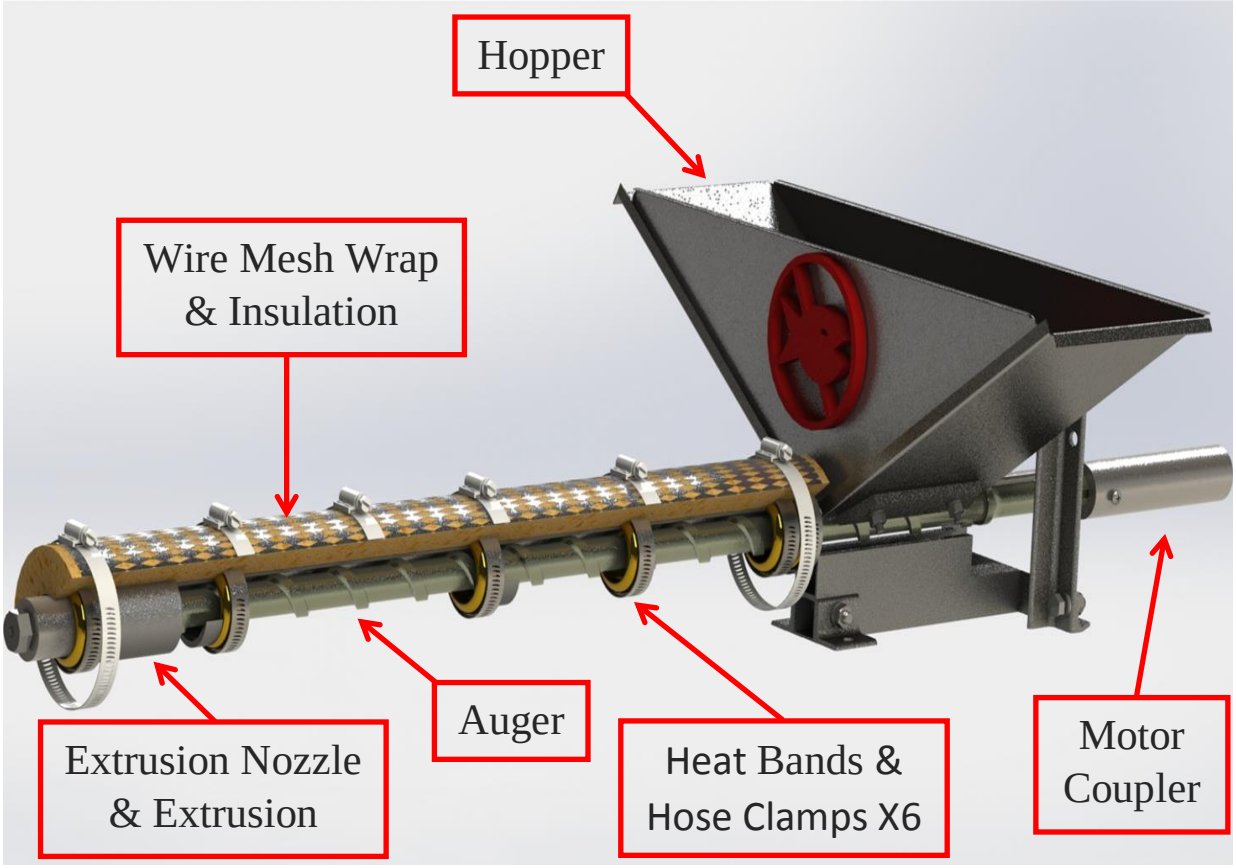

Figure 4 Heat Extrusion Unit Final Design

Thermal Distribution

The use of an infrared camera aided in Heat Band location to develop the temperature contour for the processing portion of the HEU system. Through various configurations, optimal heat distribution across the cylinder chamber was determined as seen in Figure 5. In efforts to ensure constant heat flow, thermal paste and fiberglass insulation was added to the outer surface of the pipe. With the cylinder chamber having an approximately equal temperature contour, plastic flowing through the system will maintain its intended processing speed.

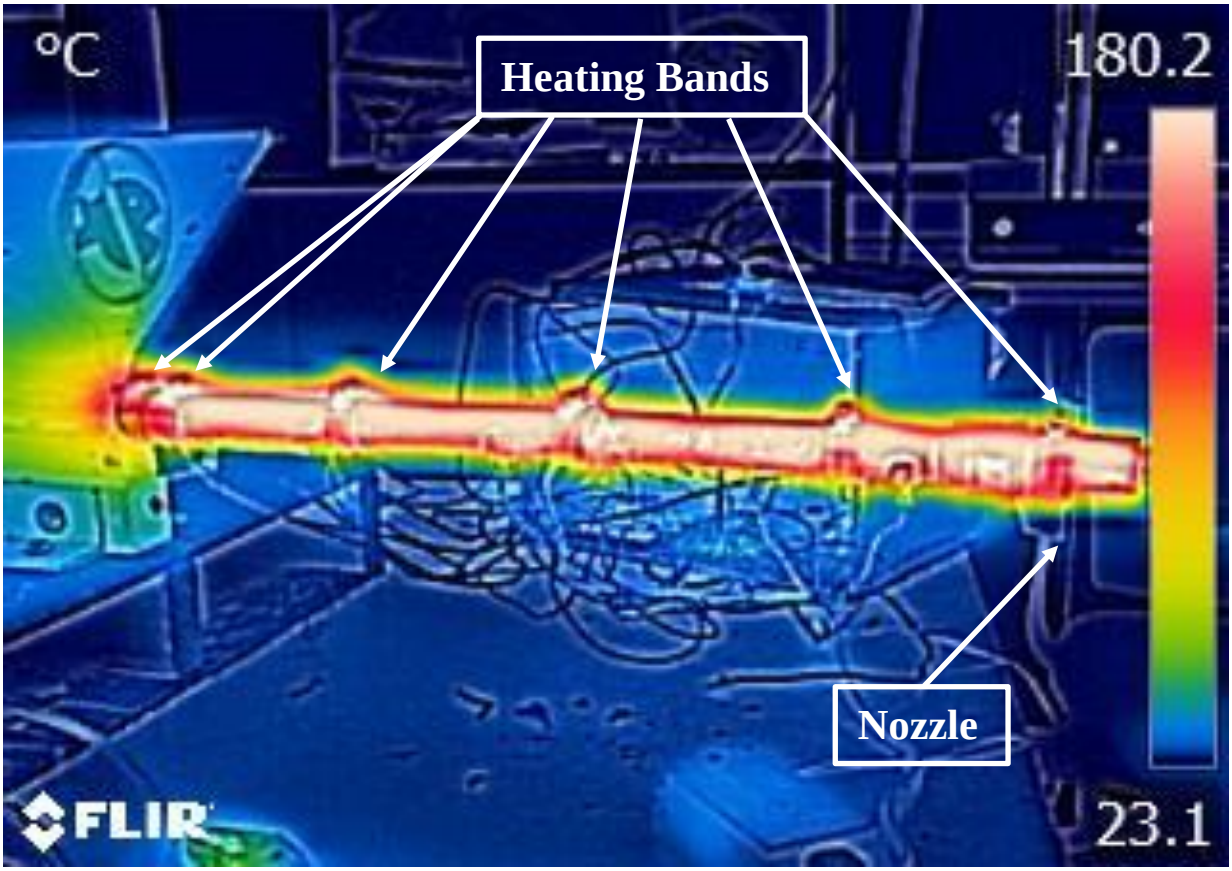

Figure 5 Thermal Distribution from Heat Bands

Deflection Analysis

An analysis to measure structural integrity of the HEU was performed on the Cylinder Chamber. The analysis was conducted to determine if the HEU was in need of support to prevent excessive deflection at the Extrusion Nozzle exit. To ease calculation difficulty, the Cylindrical Chamber was treated as a cantilever beam with a solid circular cross-section. The model created using computer aided design (CAD), had a diameter of 0.0254m, a length of 0.589m, a distributed force of 74.75 N/m, and a thermal stress of 300°C; which were identical parameters of the full scale HEU prototype. The distributed force was determined by calculating the weight of all materials from both the HEU and plastic passing through the system; whereas the chosen thermal stress was from the intended operating temperature. The results of the deflection simulation can be seen in Figure 6 with green arrows representing the fixed end, purple arrows representing the distributed force, and orange arrows representing thermal stress.

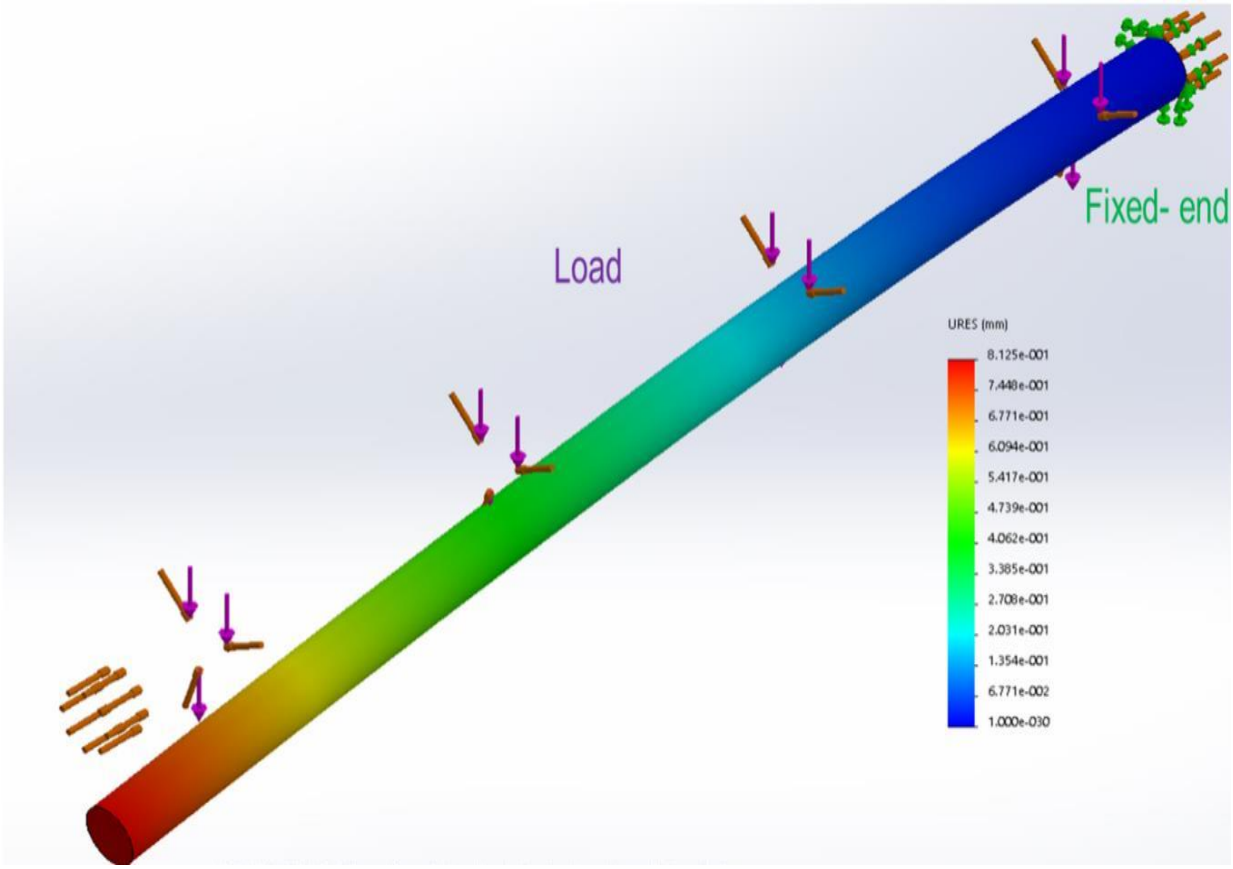

Figure 6 Deflection Simulation

This simulation concluded that with a resulting maximum deflection of 0.81mm, the Extrusion Nozzle exit end of the HEU did not require support.

Temperature Effects on Stainless-Steel

The operating temperature of the thermal bands on the extrusion cylinder chamber and Auger is throttled at a maximum 300°C. The tensile strength of 316 stainless steel, shown as upright triangles in Figure 7, is minimally affected by temperatures below 400°C; therefore, the life expectancy and survivability of the extrusion cylinder will not be effected due to temperature. Furthermore, the only factor to determine the life expectancy of stainless steel before maintenance or replacement is due to pitting. The life expectancy of 316 stainless steel under marine conditions is 260 years [9], which means minimal maintenance is required for the HEU to be self-sustained. Due to the resilience of high temperatures on tensile strength coupled with the life expectancy under marine conditions, 316 stainless steel was the preferred material to use.

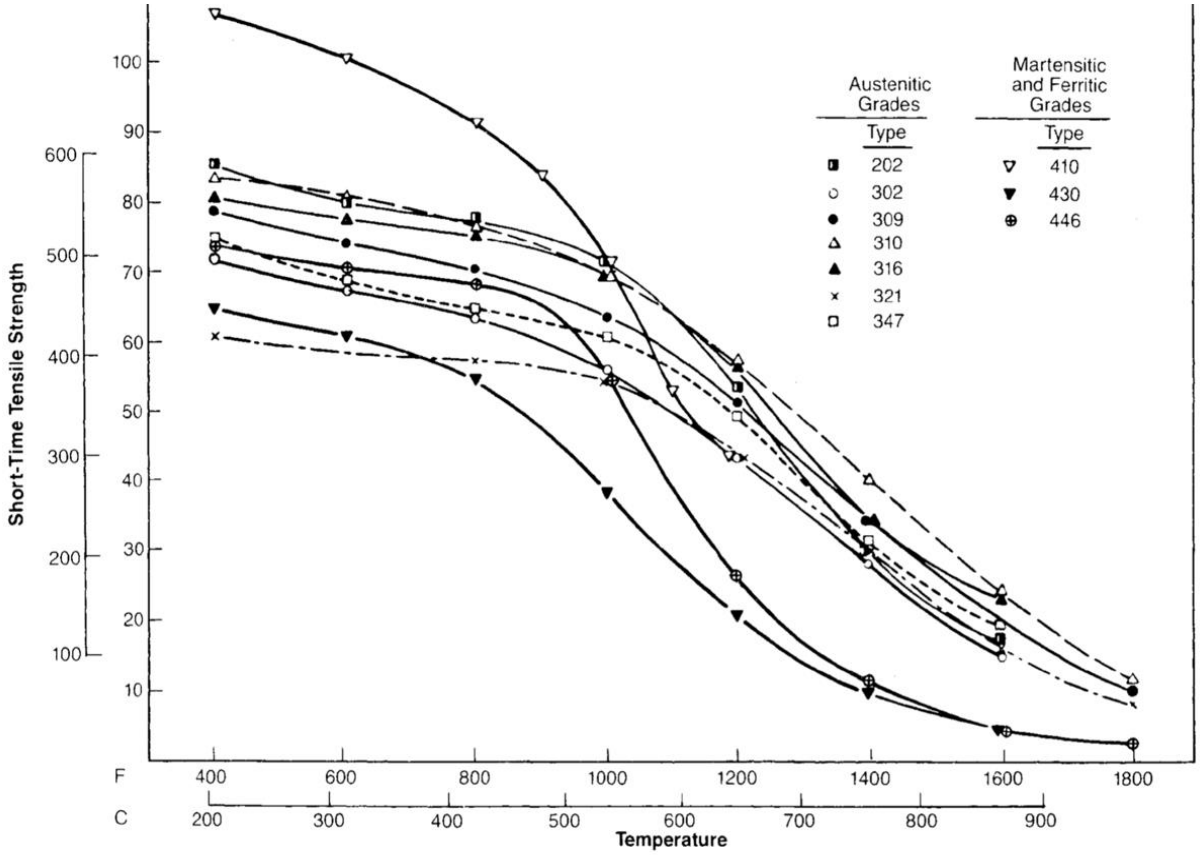

Figure 7 Thermal Effects on Stainless Steel's Tensile Strength [10]

Test Results:

Component and Assembly Weight

The overall mass and envelope size was a continuous concern during conceptual design. Prior to manufacturing and assembly, CAD was used all throughout the design process to provide numerical tabulations for the system's total weight. With a complete HEU CAD model indicating the overall mass constraint had not been exceeded, manufacturing and fabrication began. The HEU is comprised of three major sub-assemblies as seen in Figure 8 below, and its respective weights as seen in Table 2.

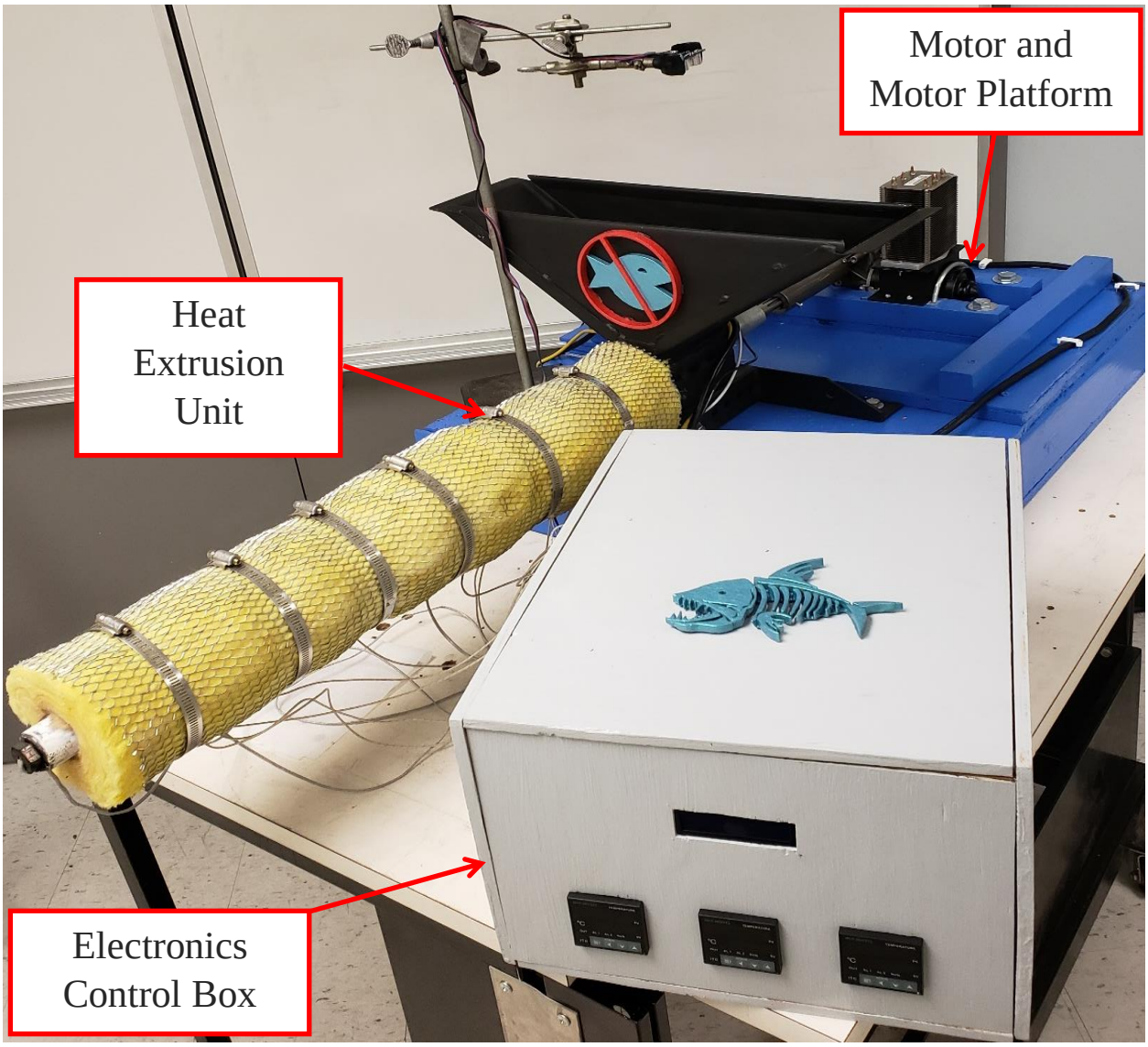

Figure 8 Heat Extrusion Unit Prototype

Table 2 Heat Extrusion Unit Weight Data

No.	Sub-Assembly Components	Weight (kg)
1	Heat Extrusion Unit	12.5
2	Motor, and Motor Platform	6.9
3	Electronics Control Box	4.8
	Total Weight =	**24.2**

Based on the 50kg or less system requirement, the percent difference of the entire system weight was 69.5%.

Power Analysis

Given the electrical components used which included Heat Bands, PIDs, a DC motor, and an Arduino, the approximate theoretical power consumption is 691.5W. Manufacture specifications can be seen in Table 3 below.

Table 3 Electrical Component Power Specifications

Component (Qty.)	Equation	Power (W)
Heat Bands (6)	100W × 6	600
PID (3)	5W×3	15
Arduino Mega (1)	10 W×1	10
DC Motor (1)	18.98 Nm × 3.46 rad/s	65.67
Relays (3)	5 V×0.04 Amps×3	0.6
LCD	5 V×0.04 Amps	0.2
	Total Power =	691.5

A Watt-meter was employed to gather data on the total power consumed during a test cycle of one hour. Both theoretical and measured power usage can be seen in Figure 9 below.

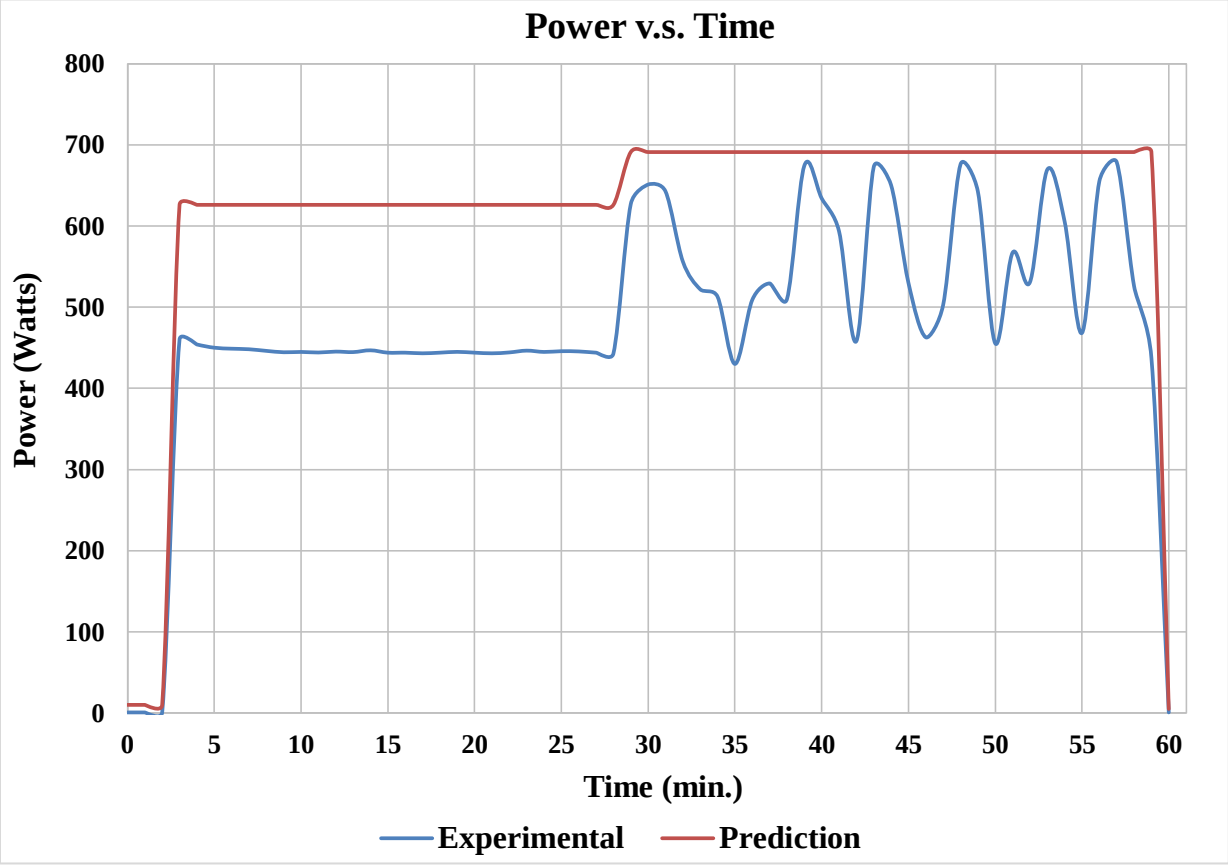

Figure 9 One-Hour Cycle of Power Consumption

The first initial rise in power between 2-5 minutes is explained by the PID's turning on and allowing current to pass through to the Relays. From 3-28 minutes, the power consumption remained stable while the chamber heated up to the pre-set Heat Band temperature. The second rise in power occurred between 27-30 minutes, when the thermocouple read the Cylindrical Chamber's internal 110°C desired glass transition temperature; causing the motor to turn on and begin plastic processing. Power fluctuations between 30-54 minutes was caused by throttling temperature, and the condition of a non Steady-State mass flow rate system.

As the Hopper became empty, power to the PIDs, motor, and Heat Bands were cut off as seen from 59-60 minutes. The HEU will constantly idle at a minimum of 5W, such that the microcontroller can receive signals from the ultrasonic sensor to repeat its plastic processing operation; as the Hopper refills.

After a one-hour power cycle, the maximum power recorded on an average was 678W, which was less than the estimated max power of 691W. Those results lead to a percent variance of approximately 2%, and a 16.5% difference between system requirement and actual usage.

Autonomy

Various electrical components were implemented in the HEU design to make it autonomous. An ultrasonic sensor was used to help determine the amount of plastic collected inside the Hopper by measuring its distance from empty to full, then relaying that information to an Arduino which functioned as a microcontroller. The PID controllers and thermocouples aided in maintaining a constant temperature throughout the Cylindrical Chamber. As the Hopper neared empty, the microcontroller would cut power to the relays and shut off all components except the Ultrasonic Sensor; which continuously monitored the Hopper's plastic depth.

Mass Flow Rate Analysis

Upon final assembly of the HEU prototype, tests to collect data for the mass flow rate was conducted. A scale was placed below the nozzle exit to record processed plastic weight, and a stop-watch to record time. After a one-hour period, the data collected revealed that this system was capable of producing 3.23kg/hr.

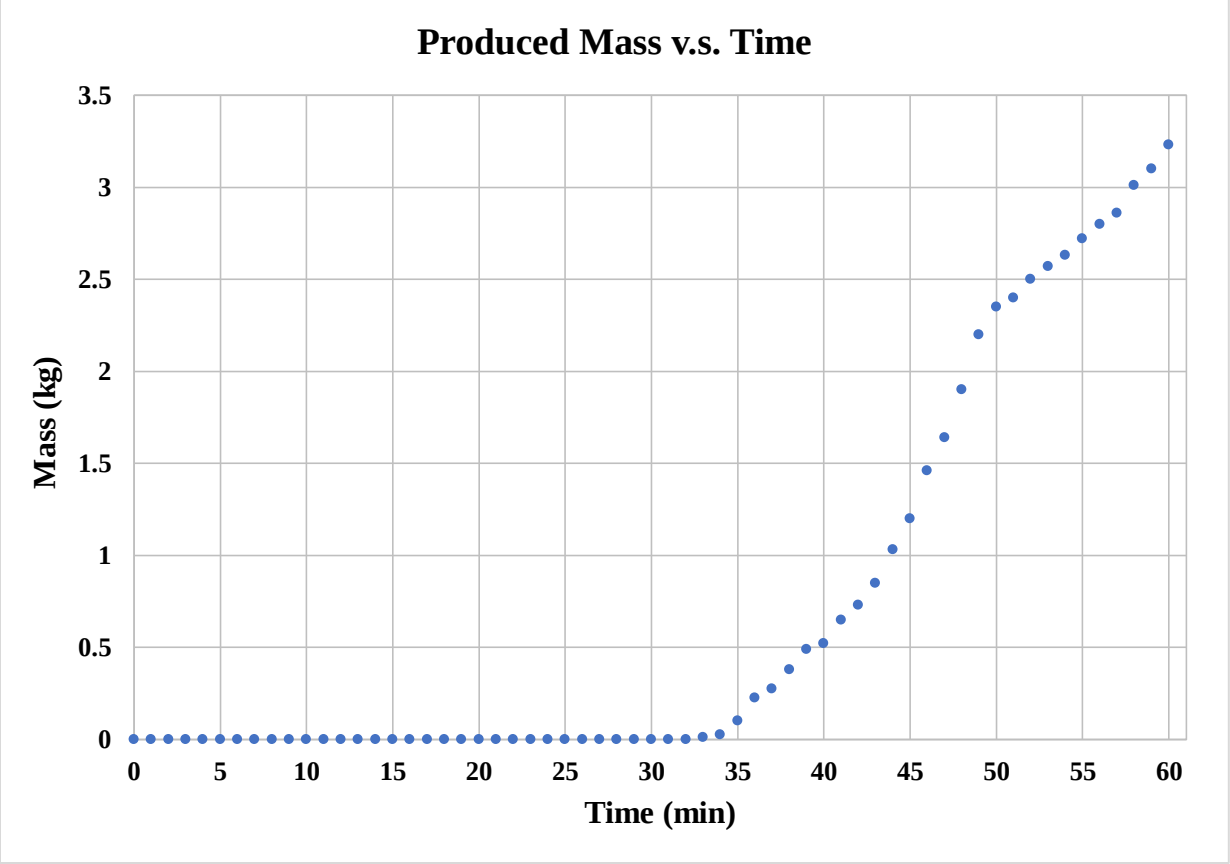

Figure 10 One-Hour Cycle of Produced Mass

With minimal to no empirical data available to theoretically model an extrusion system, theoretical angular velocity remained unknown. Using numerical analysis and setting $\dot{Q}_{md}$ equal to the system requirement of 3.63kg/h, an output of 33rpm was obtained. With the HEU's Auger angular velocity operating with a motor ouput of 33rpm, test data as seen in Figure 10 above led to a calculated percent difference between theoretical and empirical dry-plastic mass flow rate of 9%.

Discussion:

The HEU was shown to have different processing rates during testing due to the condition of the plastic. When the plastic was wet with sea-water, the processing rate was as slow as 0.82kg/h; and as fast as 3.23kg/h when the plastic was dry. The difference in processing rates is explained by the presence of different heat capacities. When the plastic is wet with sea-water, the heat capacity is 3,850 J/kg°C [11] as compared to when the plastic is dry the heat capacity is 1,030 J/kg°C [12]. As heat capacity increases, as too does the amount of energy required to raise the temperature of a material. To achieve maximum processing rate at minimum power usage for the desired glass transition temperature, the plastic entering the Hopper should be dry.

The motor used for testing provided a maximum torque of 18.98Nm at a maximum speed of 33rpm. Under dry plastic conditions, a system power requirement of 800Wh or less, and a 16.5% difference from actual power usage; utilizing the resulting percent difference by incorporating a more powerful motor will yield quicker processing rates.

Conclusion:

The Heat Extrusion Unit successfully demonstrated its abilty to process and extrude a variety of micro-sized plastic pieces. As intended, the HEU received, processed, and binded plastic pieces into larger lumps that is more manageable to handle. The HEU cycled through multiple design revisions and is supported by engineering calculations. Engineering software was used to help design, simulate, and verify test results. Although the motor was under powered to meet the 3.63kg/h system requirement, calculations have determined that a more powerful motor will produce the required mass flow rate; while not exceeding the system power constraint. Arduino was used as a microcontroller to make the system autonomous by programming it to read data such as distance from an ultrasonic sensor, and temperature from the thermocouples. A lower grade stainless steel was used during testing, however due to environmental conditions; the HEU is intended to be constructed of 316 stainless steel due to its mechanical properties which enable it to withstand corrosion caused by sea-water.

References

[1] National Oceanic and Atmospheric Administration, "Marine Debris Program," [Online]. Available: https://marinedebris.noaa.gov/info/plastic.html. [Accessed 2018].

[2] L. Parker, "Ocean Life Eats Tons of Plastic—Here's Why That Matters," National Geographic, 16 August 2017. [Online]. Available: https://news.nationalgeographic.com/2017/08/ocean-life-eats-plastic-larvaceans-anchovy-environment/.

[3] R. Manning, "Ocean Cleanup Project White Paper," 2017. [Online]. Available: https://www.raymanning.com/ocean/.

[4] J. W. Fisher and J. M. Lee, "Space Mission Utility and Requirements for a Heat Melt Compactor," *46th International Conference on Environmental Systems,* pp. 1 - 20, 2016.

[5] R. S. Li and J. Jiao, "The Effects of Temperature and Aging on Young's Moduli of Polymeric Based Flexible Substrates," *The International Journal of Microcircuits and Electronic Packaging,* vol. 23, no. 4, 2000.

[6] Y. A. Çengel and A. J. Ghajar, Heat and Mass Transfer : Fundamentals & Applications, New York: McGraw Hill Education, 2015.

[7] C. Borgnakke and R. E. Sonntag, Fundamental of Thermal Dynamic, 8th ed., Hoboken: John Wiley and Sons, 2013.

[8] G. Campbell and M. Spalding, Single-Screw Extrusion: Introduction and Troubleshooting, 2013.

[9] American Iron and Steel Institute, High-temperature Characteristics of Stainless Steels, Committee of Stainless Steel Producers, American Iron and Steel Institute, 1979.

[10] British Stainless Steal Association, "Durability and life expectancy for stainless steels in external environments," [Online]. Available: https://www.bssa.org.uk/topics.php?article=51. [Accessed 2018].

[11] L. Talley, "Properties of Seawater," [Online]. Available: http://sam.ucsd.edu/sio210/lect_2/lecture_2.html. [Accessed 2018].

[12] The Engineering Toolbox, "Polymers-Specific Heat," [Online]. Available: https://www.engineeringtoolbox.com/specific-heat-polymers-d_1862.html. [Accessed 2018].